RESEARCH ARTICLE

PLANT SCIENCE

A paralogous decoy protects *Phytophthora sojae* apoplastic effector PsXEG1 from a host inhibitor

Zhenchuan Ma,[1,2] Lin Zhu,[1,2] Tianqiao Song,[1,2] Yang Wang,[1,2] Qi Zhang,[1,2] Yeqiang Xia,[1,2] Min Qiu,[1,2] Yachun Lin,[1,2] Haiyang Li,[1,2] Liang Kong,[1,2] Yufeng Fang,[3] Wenwu Ye,[1,2] Yan Wang,[1,2] Suomeng Dong,[1,2] Xiaobo Zheng,[1,2] Brett M. Tyler,[3] Yuanchao Wang[1,2]*

The extracellular space (apoplast) of plant tissue represents a critical battleground between plants and attacking microbes. Here we show that a pathogen-secreted apoplastic xyloglucan-specific endoglucanase, PsXEG1, is a focus of this struggle in the *Phytophthora sojae*–soybean interaction. We show that soybean produces an apoplastic glucanase inhibitor protein, GmGIP1, that binds to PsXEG1 to block its contribution to virulence. *P. sojae*, however, secretes a paralogous PsXEG1-like protein, PsXLP1, that has lost enzyme activity but binds to GmGIP1 more tightly than does PsXEG1, thus freeing PsXEG1 to support *P. sojae* infection. The gene pair encoding PsXEG1 and PsXLP1 is conserved in many *Phytophthora* species, and the *P. parasitica* orthologs PpXEG1 and PpXLP1 have similar functions. Thus, this apoplastic decoy strategy may be widely used in *Phytophthora* pathosystems.

Plants have evolved innate immune systems that are capable of recognizing potential invading pathogens and initiating effective defense responses (*1*, *2*), whereas successful pathogens have developed effector proteins that can suppress host immune responses (*3*–*5*). Effector-triggered susceptibility can be a result of the activities of apoplastic (extracellular) or cytoplasmic (intracellular) effectors (*6*, *7*). Early interactions between plant pathogens and their hosts take place in the apoplast (*8*, *9*). Both pathogens and plants secrete antagonistic compounds into the apoplast, including hydrolytic enzymes, enzyme inhibitors, enzymes to increase and decrease reactive oxygen species, and antimicrobial proteins and metabolites. Plants also monitor the apoplastic environment through pattern recognition receptors that can detect fragments of pathogen molecules (pathogen-associated molecular patterns, or PAMPs) (*5*).

Oomycetes, a lineage of eukaryotic microorganisms in the kingdom Stramenopila, include pathogens of plants and animals (*5*, *10*, *11*). Among these, many destructive pathogens of crops are in the genus *Phytophthora* (*11*–*13*). Some species, such as *Phytophthora sojae*, the agent of soybean (*Glycine max* L.) root and stem rot, have caused long-standing problems for agriculture (*12*). During infection, oomycetes secrete glycoside hydrolases such as the xyloglucan-specific endoglucanase PsXEG1. PsXEG1 is an essential virulence effector that functions in the apoplast and is recognized by the plant's PAMP recognition machinery. That recognition does not depend on the enzymatic activity of PsXEG1, which is to hydrolyze xyloglucan and β-1,4-glucan to reducing sugars (*14*). Here we show that the pathogen protects PsXEG1 from a host inhibitor by means of a more tightly binding protein paralog.

[1]Department of Plant Pathology, Nanjing Agricultural University, Nanjing 210095, China. [2]Key Laboratory of Integrated Management of Crop Diseases and Pests (Ministry of Education), Nanjing 210095, China. [3]Center for Genome Research and Biocomputing and Department of Botany and Plant Pathology, Oregon State University, Corvallis, OR 97331, USA.
***Corresponding author. Email: wangyc@njau.edu.cn**

Soybean GmGIP1 binds *P. sojae* xyloglucanase PsXEG1 and inhibits its enzyme activity

To identify potential host inhibitors of PsXEG1, we isolated total proteins from *P. sojae*–inoculated soybean hypocotyls. Then we incubated those proteins with PsXEG1–green fluorescent protein (GFP) fusion protein and captured the protein complexes on GFP-trap beads. The captured proteins were analyzed by tandem mass spectrometry. We detected a protein with 37% amino acid identity to the tomato xyloglucan-specific endoglucanase inhibitor protein XEGIP (*15*), which we named soybean glucanase inhibitor protein 1 (GmGIP1) (table S1). We confirmed the interactions between PsXEG1 and GmGIP1 by reciprocal coimmunoprecipitation (co-IP) assays of proteins transiently coexpressed in *Nicotiana benthamiana* (fig. S1A). Like other GIPs, GmGIP1 has similarity to aspartate proteases, but it lacks a critical catalytic aspartate residue (*16*). Accordingly, no instability of PsXEG1 was detected when coexpressed with GmGIP1 in *N. benthamiana* (fig. S1A). To test whether PsXEG1 and GmGIP1 could bind each other directly, we performed in vitro pull-down assays of PsXEG1 expressed in *Pichia pastoris*, using GmGIP1 expressed in *Escherichia coli*. The pull-down assays showed that PsXEG1 directly bound GmGIP1 (fig. S1B). Moreover, screening of other GmGIP1 paralogs for PsXEG1 binding, using transient expression assays in *N. benthamiana*, showed that the PsXEG1-GmGIP1 interaction was specific (fig. S1C); no GmGIP1 paralogs bound PsXEG1.

To ascertain which amino acids determined the binding of GmGIP1 to PsXEG1, the interacting proteins were modeled using the crystal structure (3VLB) of the complex of carrot EDGP1 with *Aspergillus* xyloglucanase (*16*). The model suggested that GmGIP1 might bind to PsXEG1 through five regions, G1 to G5 (fig. S2A). Alanine substitution mutations in each of the five regions were tested for their ability to disrupt the interaction of GmGIP1 with PsXEG1 (fig. S2, B and C). In planta co-IP assays revealed that mutations in G5, which spans nine amino acids of GmGIP1 (positions 408 to 416), almost abolished the interaction with PsXEG1. In addition, G1 (position 196), G2 (position 210), and G3 (positions 324 to 330) were also required for full binding activity.

We next investigated whether GmGIP1 could inhibit the hydrolysis of xyloglucans by PsXEG1 (*16*). Increasing amounts of purified GmGIP1 protein strongly inhibited PsXEG1-catalyzed depolymerization of xyloglucan in vitro, compared with the effects of the GmGIP1^{G5} mutant, as monitored by the release of reducing sugars (Fig. 1A). The lower activity of PsXEG1 was not due to instability caused by GmGIP1, because PsXEG1 protein remained stable after a 6-hour incubation in the presence of GmGIP1 (fig. S3). These results suggested that GmGIP1 could function as an inhibitor of PsXEG1's xyloglucanase activity.

GmGIP1 inhibits PsXEG1's contribution to *P. sojae* virulence

To address the contribution of GmGIP1-mediated inhibition of PsXEG1 to host resistance against *P. sojae*, we generated transgenic soybean hairy roots in which *GmGIP1* or mutant *GmGIP1*^{G5} was overexpressed or the *GmGIP1* gene was silenced (fig. S4, A to D). Quantitative reverse transcription polymerase chain reaction (qRT-PCR) analysis of *GmGIP1*-silencing lines revealed a selective reduction of *GmGIP1* transcripts, but not of transcripts of paralogous genes (*Gm148200* and *Gm210100*) (fig. S4E). These transgenic soybean roots showed normal morphology and development compared with the control lines expressing GFP or RNA interference empty vector (RNAi EV). In response to pathogen challenge, compared with transgenic lines expressing *GFP* or the *GmGIP1*^{G5} mutant, all of the *GmGIP1*-silenced transgenic plants displayed significantly increased susceptibility, whereas all of the *GmGIP1*-overexpressing lines showed increased resistance, as evidenced by genomic DNA qPCR analysis of pathogen biomass and the quantity of oospores produced (Fig. 1, B and C, and fig. S4F). Transcript levels of other defense

genes in these lines were not significantly different from those in plants expressing *GFP* (fig. S5). These results indicated that GmGIP1 contributes positively to soybean resistance against *P. sojae*, presumably as a result of inhibition of PsXEG1. This conclusion was further supported by the observation that pretreatment of *P. sojae* zoospores with the GmGIP1 protein reduced the pathogen's virulence on etiolated soybean hypocotyls (Fig. 1D and fig. S6).

PsXEG1's contribution to virulence requires its enzyme activity

Given these findings and the inhibitory effect of GmGIP1 on PsXEG1, we used Cas9-mediated homologous gene replacement in *P. sojae* (*17*) to confirm that the virulence contribution of PsXEG1 requires its hydrolytic activity (*14*). We generated homozygous *PsXEG1* deletion lines and lines in which *PsXEG1* was replaced with *GUS* or with the *PsXEG1*^{E136D,E222D} catalytic-site mutant (abbreviated *PsXEG1*$^{EE\rightarrow DD}$; E, glutamic acid; D, aspartic acid) (figs. S7 and S8A). All transformants showed normal filamentous growth (fig. S8, B and C). Both knockout of *PsXEG1* and its replacement by *GUS* reduced *P. sojae* virulence in soybean (fig. S8, D and E). Moreover, the catalytic-site mutant lines infected soybean no better than the *PsXEG1* knockout lines or the *GUS* replacement lines. This result confirmed that *P. sojae* depends on PsXEG1's hydrolytic activity for full virulence.

PsXLP1, a truncated paralog of *P. sojae* PsXEG1, binds GmGIP1

To determine whether GmGIP1 might inhibit other PsXEG1 family members, we performed co-IP assays of transiently expressed PsXEG1 paralogs in *N. benthamiana*. Of 10 paralogs tested, only one, named *P. sojae* XEG1-like protein 1 (PsXLP1), showed an interaction with GmGIP1 (fig. S9). PsXLP1 had ~67% amino acid sequence identity with PsXEG1 (fig. S10B). However, PsXLP1 was 52 residues shorter than PsXEG1 because of a deletion near the C terminus that created a frameshift mutation, resulting in the loss of one of the residues critical for enzyme activity (E222). Like PsXEG1, PsXLP1 was secreted from *P. sojae* overexpression lines (fig. S11A), indicating that both proteins are targeted to the apoplast. GmGIP1 was likewise secreted after transient expression in *N. benthamiana* (fig. S11B).

We assessed the hydrolase activity of PsXLP1 by determining the level of reducing sugars in the apoplastic fluid of *N. benthamiana* leaves transiently expressing PsXLP1. There were no significant differences compared with levels in tissues expressing the negative controls GFP, PsXEG1^{E136D}, or PsXEG1^{E222D}. However, the reducing sugars were elevated in the apoplastic fluid of *N. benthamiana* leaves transiently expressing PsXEG1 (fig. S12). These results suggested that PsXLP1 lacks hydrolase activity comparable to that of PsXEG1, although we cannot rule out that the substrates of PsXLP1 were absent in this assay.

To identify the amino acids of PsXLP1 required for binding GmGIP1, we compared structural models of the PsXEG1-GmGIP1 and PsXLP1-GmGIP1 complexes based on the 3VLB structure (*16*). Five regions of PsXLP1 (X1 to X5) were predicted to interact with GmGIP1, in which some interacting residues were shared with PsXEG1 and some differed (fig. S10). Next, alanine substitution mutations in each of the five regions were tested for their ability to disrupt the interaction with GmGIP1. Co-IP assays of transiently expressed PsXLP1 mutants with GmGIP1 in *N. benthamiana* revealed that X1 (position 26), X2 (positions 39 to 44), X3 (positions 77 and 78), and X5 (positions 146 to 150) were all required for full binding activity of PsXLP1 to GmGIP1 (fig. S13).

PsXLP1's contribution to *P. sojae* virulence requires GmGIP1 binding, but not enzyme activity

To explore the possible contribution of *PsXLP1* to *P. sojae* virulence, we determined the expression pattern of *PsXLP1* during different stages of development. *PsXLP1* was strongly expressed at high levels during very early infection stages (20 min to 2 hours) and then rapidly declined from 3 hours onward (Fig. 2A), which suggested that *PsXLP1* might contribute to *P. sojae* virulence. Moreover, the expression pattern of *PsXLP1* was strongly correlated with that of *PsXEG1* (Fig. 2A). Furthermore, the *PsXEG1* and *PsXLP1* genes were closely located 2370 base pairs (bp) apart in the *P. sojae* genome, in a head-to-head arrangement, suggesting regulation by a common element (Fig. 2B). Because *PsXEG1* homologs are widely distributed across microbial taxa (*14*), we looked for *PsXLP1* homologs in the genomes of 12 oomycete, three fungal, and one bacterial species. *PsXLP1* orthologs were present in almost all the sequenced *Phytophthora* species, and, in every case where they were present, were arranged head-to-head with the *PsXEG1* ortholog (fig. S14). However, close comparison of the *P. sojae PsXLP1* DNA sequence with the orthologs in other species revealed that the *P. sojae PsXLP1* gene had been modified very recently by a gene conversion from *PsXEG1* encompassing nucleotide positions ~130 to 530. In addition, two deletions of 68 and 5 bp beginning at position 534 had created a frameshift mutation that resulted in a stop codon at position 562 (figs. S15 and S16).

To test the contribution of *PsXLP1* to *P. sojae* virulence, we replaced *PsXLP1* with no sequence (a complete deletion) or with *GUS* by Cas9-mediated homologous gene replacement. In addition, we overexpressed *PsXLP1* by transformation of *P. sojae* with sense constructs driven by the strong constitutive *HAM34* promoter (figs. S17, S18A, and S18B) (*18*). All the transformed lines showed normal morphology and development (fig. S18, C and D). Both knockout of *PsXLP1* and its replacement by

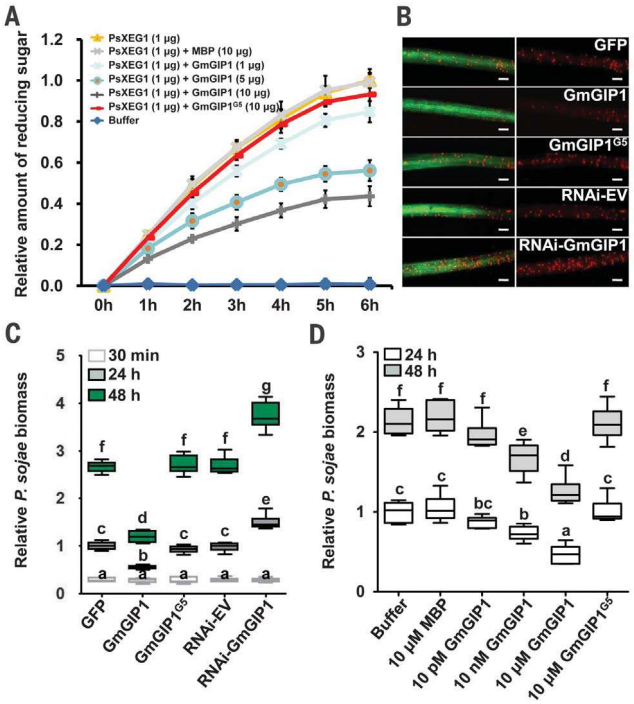

Fig. 1. GmGIP1, a host inhibitor of PsXEG1, contributes to resistance against *P. sojae*. (**A**) PsXEG1 activity in the presence of GmGIP1 was measured in vitro by the release of reducing sugar over time, normalized to 1 μg of PsXEG1 at 6 hours. Values are means ± SEM of three independent biological replicates. MBP, maltose-binding protein. (**B** and **C**) Expression levels of GmGIP1 in soybean hairy roots affect defense against *P. sojae*. Transgenic hairy roots expressing GFP and either elevated GmGIP1, GmGIP1^{G5} mutant, or a *GmGIP1*-silencing construct (GmGIP1 RNAi or EV control) were inoculated with *P. sojae* zoospores expressing red fluorescence protein (RFP). Levels of GmGIP1 protein and transcripts in the hairy roots are shown in fig. S4. Oospore production at 48 hours postinoculation (hpi) is shown in (B). Six independent experiments gave similar results. Left, merged (RFP + GFP); right, RFP. Scale bars, 0.2 mm. Shown in (C) is the relative biomass of *P. sojae* in infected hairy roots, measured by genomic DNA qPCR and normalized to the GFP control at 24 hpi (six replicates, each consisting of a total of 36 hairy roots from 6 cotyledons). (**D**) In vitro treatment of *P. sojae* with GmGIP1 protein decreased infection. Relative *P. sojae* biomass in infected etiolated hypocotyls (after treatment with indicated proteins) was measured by genomic DNA qPCR and normalized to buffer control at 24 hpi (seven replicates). In (C) and (D), different letters represent significant differences ($P < 0.01$; Duncan's multiple range test). Bars represent medians, and boxes indicate the 25th and 75th percentiles.

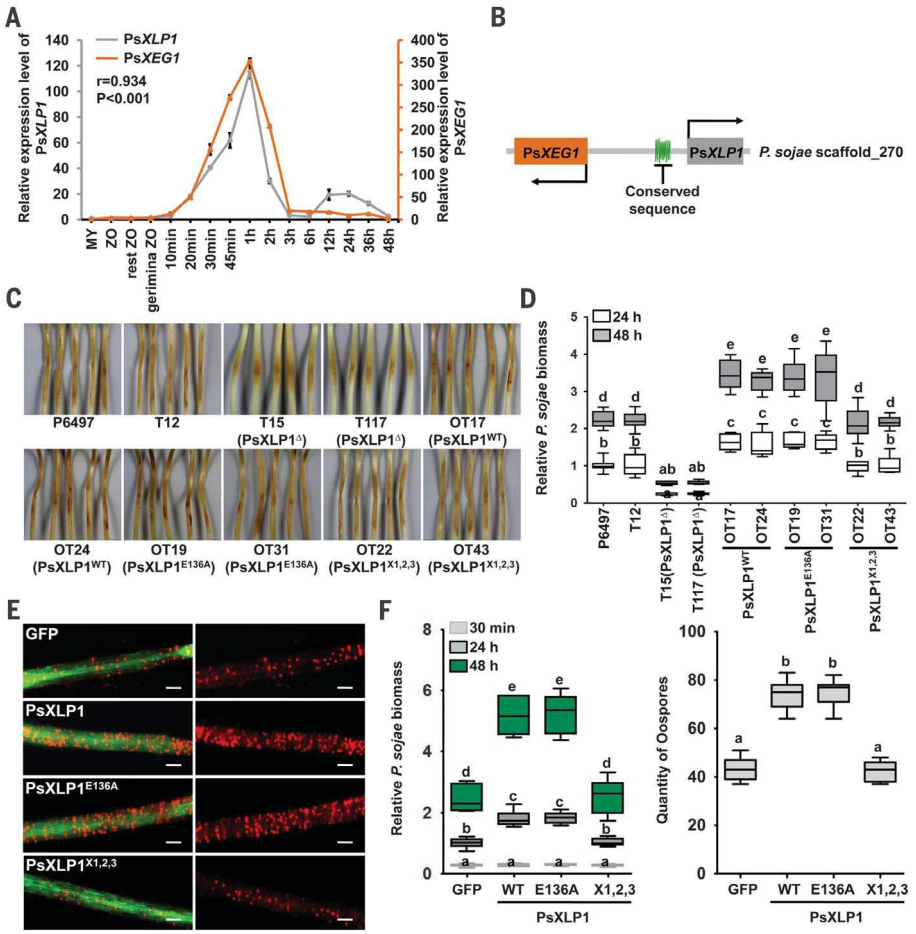

Fig. 2. PsXEG1 paralog PsXLP1 requires a GmGIP1-binding site, but not a catalytic site, to contribute to virulence. (**A**) *PsXLP1* and *PsXEG1* transcript levels are closely correlated, as measured by qRT-PCR. My, mycelium; Zo, zoospores; infected soybean, 10 min to 48 hours. Values are means ± SEM of three independent experiments. (**B**) Head-to-head organization of the *PsXEG1* and *PsXLP1* genes in *P. sojae*. Green area, sequence conserved in *Phytophthora* genomes. (**C** and **D**) Overexpression or replacement of *PsXLP1* in *P. sojae* influences virulence on etiolated soybean hypocotyls. P6497, wild type (WT); *PsXLP1*$^{\Delta}$, deletion; OT, overexpression; T12, control; XLP1, overexpressed mutant; PsXLP1^{E136A} and PsXLP1^{X1,2,3}, mutations in predicted catalytic and GmGIP1-binding residues, respectively (fig. S10). Representative symptoms at 48 hpi from six independent experiments are shown in (C). Relative *P. sojae* biomass in infected soybean, measured by genomic DNA qPCR, is shown in (D). (**E** and **F**) Expression of PsXLP1 in soybean hairy roots influences susceptibility to *P. sojae*. Hairy roots were inoculated with zoospores expressing RFP. Shown in (E) is oospore production at 48 hpi, representative of six independent experiments, each consisting of a total of 30 hairy roots from 5 cotyledons. Left, merged (RFP + GFP); right, RFP. Scale bars, 0.2 mm. *P. sojae* biomass and oospore abundance in infected roots are shown in (F). Six replicates were used, each consisting of a total of 36 hairy roots from 6 cotyledons for *P. sojae* biomass. In (D) and (F), different letters represent significant differences ($P < 0.01$; Duncan's multiple range test). Bars represent medians, and boxes indicate the 25th and 75th percentiles.

GUS resulted in severely restricted *P. sojae* infection, whereas all of the *PsXLP1*-overexpressing lines exhibited increased virulence in soybean (Fig. 2, C and D, and fig. S18, E and F). These results indicated that PsXLP1 plays a positive role in *P. sojae* virulence. This conclusion was supported by the observation that *PsXLP1* expression in soybean roots could promote susceptibility to *P. sojae* (Fig. 2, E and F, and fig. S19). Taken together, these results showed that PsXLP1 is a major virulence factor for *P. sojae*.

To dissect the mechanism by which PsXLP1 contributes to virulence, two additional *PsXLP1* mutants were generated. *PsXLP1*^{E136A} contains a mutation in the remaining theoretical active-site residue glutamate (E136; A, alanine). *PsXLP1*^{X1,2,3} combines mutations in the binding site regions X1, X2, and X3 (figs. S10 and S13). In planta co-IP assays revealed that PsXLP1^{X1,2,3} bound very weakly to GmGIP1, but PsXLP1^{E136A} bound to GmGIP1 as strongly as wild-type PsXLP1 did (fig. S13). Transgenic *P. sojae* lines overexpressing ectopic *PsXLP1*^{E136A} or *PsXLP1*^{X1,2,3} genes were generated (fig. S18, A and B) and assayed for virulence in soybean. Compared with the wild-type (P6497) and negative control transgenic strains, all of the PsXLP1^{E136A}-expressing transgenic *P. sojae* lines exhibited significantly increased virulence, comparable to that of lines overexpressing wild-type PsXLP1. However, none of the PsXLP1^{X1,2,3}-expressing lines displayed significant changes in terms of lesions or biomass (Fig. 2, C and D). All transgenic lines showed normal morphology and development (fig. S18, C and D). These results indicated that the residues required for GmGIP1 binding are essential for the contribution of PsXLP1 to *P. sojae* virulence, but the residue theoretically required for any PsXLP1 hydrolytic enzyme activity is not. These conclusions were further supported by experiments showing that PsXLP1^{E136A} expression in soybean roots could promote susceptibility to *P. sojae*, but expression of PsXLP1^{X1,2,3} could not (Fig. 2, E and F, and fig. S19).

PsXLP1 can protect PsXEG1 from GmGIP1 binding in vitro and in planta

Because the GmGIP1-binding activity of PsXLP1 is required for its contribution to virulence, we next tested whether the GmGIP1-PsXEG1 complex could be disrupted by PsXLP1. Co-IP of PsXEG1 and GmGIP1 was examined in *N. benthamiana* leaves expressing PsXLP1 or PsXLP1^{X1,2,3}. We observed that PsXEG1-GmGIP1 interactions were significantly reduced in the presence of PsXLP1 but were unchanged in the presence of PsXLP1^{X1,2,3} (Fig. 3A). The reduced interactions of PsXEG1 and GmGIP1 were not due to protein instability, because there were no changes in protein levels in the presence of PsXLP1 proteins (Fig. 3A). To test how PsXLP1 could displace PsXEG1 from GmGIP1 complexes, the in vitro binding affinities of GmGIP1 for PsXEG1 and PsXLP1 were determined by isothermal titration calorimetry (ITC) using purified proteins. The dissociation constants (K_d) revealed that PsXLP1 bound five times as tightly to GmGIP1 as PsXEG1 did (Fig. 3B and fig. S20). These results suggested that PsXLP1 might protect PsXEG1 from GmGIP1 binding during soybean infection.

To test whether the virulence contribution of PsXLP1 involves interference with the function of GmGIP1, we measured whether overexpression of PsXLP1 in *P. sojae* transformants could restore *P. sojae* virulence in transgenic soybean roots overexpressing GmGIP1. The transgenic *P. sojae* lines overexpressing PsXLP1 almost fully restored virulence in these roots (Fig. 4A). Moreover, the restoration of virulence depended on the GmGIP1-binding activity of PsXLP1, because PsXLP1^{X1,2,3} overexpression could not restore virulence against the transgenic soybean roots expressing GmGIP1. These results suggested that PsXLP1 overexpression in *P. sojae* could effectively counteract the resistance mediated by GmGIP1 overexpression in soybean.

PsXEG1 and PsXLP1 are both required to elevate apoplastic sugar during *P. sojae* infection

To directly determine the contribution of PsXEG1 to apoplastic sugar levels, we measured reducing sugar levels in the apoplastic fluid of soybean

leaves at various times of infection. As shown in fig. S21A, apoplastic sugar levels increased two- to threefold from 20 to 120 min postinoculation. Next, four independent *P. sojae* mutants containing deletions of the *PsXEG1* or *PsXLP1* genes were assayed for their impact on apoplastic sugar levels. The levels were measured at 30 min postinoculation, a time when the biomass of the mutants in the soybean tissue was still comparable to the levels of wild-type and control transformant strains (fig. S21B). Deletion of either *PsXEG1* or *PsXLP1* resulted in a significant ($P < 0.01$) decrease of 20% in the apoplastic reducing sugar levels (fig. S21C).

PsXLP1 contributes to *P. sojae* virulence by protecting PsXEG1 from GmGIP1 inhibition

To investigate whether PsXEG1 is required for the contribution of PsXLP1 to virulence, we performed infection assays using the *P. sojae PsXEG1* knockout lines, *GUS* replacement lines, and *PsXEG1*^{E136D,E222D} catalytic-site mutant lines on transgenic soybean roots expressing *PsXLP1* (Fig. 4B). The *P. sojae PsXEG1* mutants infected the transgenic soybean roots expressing PsXLP1 no better than the transgenic root lines expressing GFP. In contrast, wild-type P6497 and the control transformant T17 exhibited increased virulence in transgenic soybean roots expressing PsXLP1 compared with the transgenic root lines expressing GFP. These results demonstrated that the contribution of PsXLP1 to *P. sojae* virulence depends entirely on PsXEG1.

P. parasitica PpXLP1 protects PpXEG1 from binding and inhibition by *N. benthamiana* NbGIP2

The conservation of the *XEG1-XLP1* head-to-head gene pair (fig. S14) suggests that XLP1 orthologs may protect XEG1 orthologs from inhibition in many *Phytophthora* species. This possibility is supported by preliminary analysis of *PpXLP1* and *PpXEG1* in the interaction of *P. parasitica* with a host plant, *N. benthamiana*. PpXEG1 closely resembles PsXEG1 (fig. S22A), whereas *PpXLP1* encodes a full-length GH12-like protein (figs. S15 and S22B). In co-IP experiments, PpXEG1 and PpXLP1 both interacted specifically with a *N. benthamiana* GIP paralog (NbGIP2) encoded by gene model *Scf03191.g04002.1* (fig. S24, A and B). Interestingly, NbGIP2 is not orthologous to GmGIP1 (fig. S23C). Transient expression in *N. benthamiana* of PpXEG1, but not its active-site mutant PpXEG1$^{EE\rightarrow DD}$ (fig. S22A) or PpXLP1, resulted in elevated levels of reducing sugars in the apoplast (fig. S24, C and D). Coexpression of NbGIP2, but not its predicted binding-site mutant NbGIP2^{G5}, blocked the ability of PpXEG1 to raise sugar levels (fig. S24, C and D). When PpXEG1 and NbGIP2 were coexpressed, further expression of PpXLP1 or its theoretical active-site mutant PpXLP1$^{EE\rightarrow DD}$ (fig. S22B) relieved NbGIP2 inhibition of PpXEG1-induced sugar elevation, but the predicted binding-site mutant PpXLP^{X1,2,3}(fig. S22B) did not (fig. S24, C and E). In co-IP assays, PpXLP1, but not its binding-site mutant PpXLP^{X1,2,3}, displaced PpXEG1 from a complex with NbGIP2 (fig. S24F). Although the strong cell death triggered in *N. benthamiana* by PpXLP1 overexpression prevented us from assaying the ability of PpXLP1 to promote susceptibility to *P. parasitica*, the above results are consistent with a model in which PpXLP1 acts to protect PpXEG1 from inhibition by NbGIP2 during *P. parasitica* infection of *N. benthamiana*.

Discussion

Our results point to a model in which PsXLP1 has evolved as a paralogous decoy to neutralize the ability of GmGIP1 to block PsXEG1 (Fig. 4C). Our data suggest that PsXLP1 itself has no function in the development of disease, other than to intercept GmGIP1 in order to protect PsXEG1 hydrolase activity from inhibition (Fig. 4C). Our analysis of the interactions of PpXEG1 and PpXLP1 with NbGIP2 (fig. S24) suggest that this mechanism might be used by many *Phytophthora* species. The role of plant decoys—typically, proteins that resemble the target of a pathogen effector but have no function, other than as decoys—has previously been documented in the context of host innate immunity (*19*–*26*). The decoy is guarded by a Resistance (R) protein that is in some cases fused to the decoy. Binding of the effector to the decoy causes the R protein to signal effector-triggered immunity, preventing infection. Here we have shown that a pathogen, *P. sojae*, also deploys a decoy (PsXLP1) to disrupt plant defense. This protein resembles a functional virulence protein (PsXEG1) but has no function other than to act as a decoy to trap the host defense protein (GmGIP1) and neutralize it. Thus, both the host and pathogen forms of decoys are specialized paralogs of functional defense or virulence proteins, respectively, whereas the trap created by the decoy is specialized

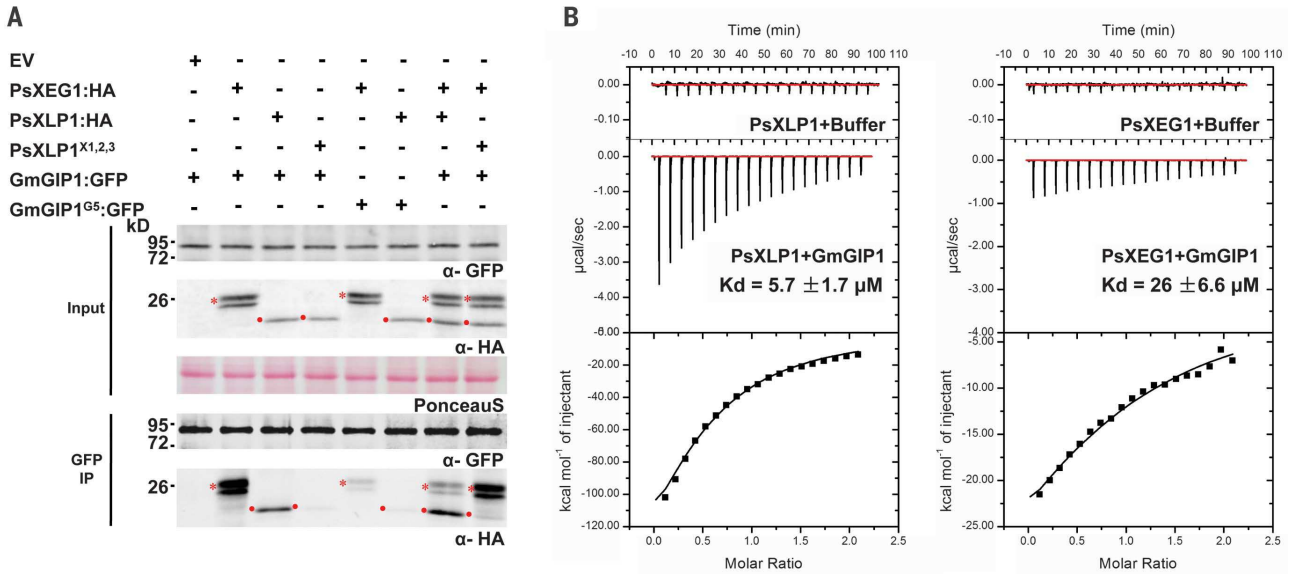

Fig. 3. PsXLP1 outcompetes PsXEG1 for GmGIP1 binding. (**A**) PsXLP1 expression disrupts GmGIP1-PsXEG1 interactions in planta. Shown are the results of co-IP of proteins transiently expressed in *N. benthamiana* leaves (representative images from three experiments). Immunoprecipitates (IPs) were analyzed by immunoblot with the indicated antibodies (α). Input fractions show equal amounts of protein for each set of IPs. Size markers (in kilodaltons) are shown on the left. Asterisks and dots indicate the expected sizes of PsXEG1 and PsXLP1, respectively. HA, hemagglutinin. (**B**) PsXLP1 exhibits stronger GmGIP1-binding affinity than PsXEG1, as assessed by ITC. PsXEG1 or PsXLP1 (204 μM) was added to buffer (upper panels) or a solution of GmGIP1-GFP fusion protein (middle panels), and the heat of binding was measured after each injection (red, base line; black, heat fluctuations). The concentration of GmGIP1 in the sample cell was 10 μM. The K_d values are the average ± the range from two independent ITC experiments. The bottom panels show integrated heats of injection (squares) and the best fit (solid line) to a single-site binding model, determined using MicroCal Origin software.

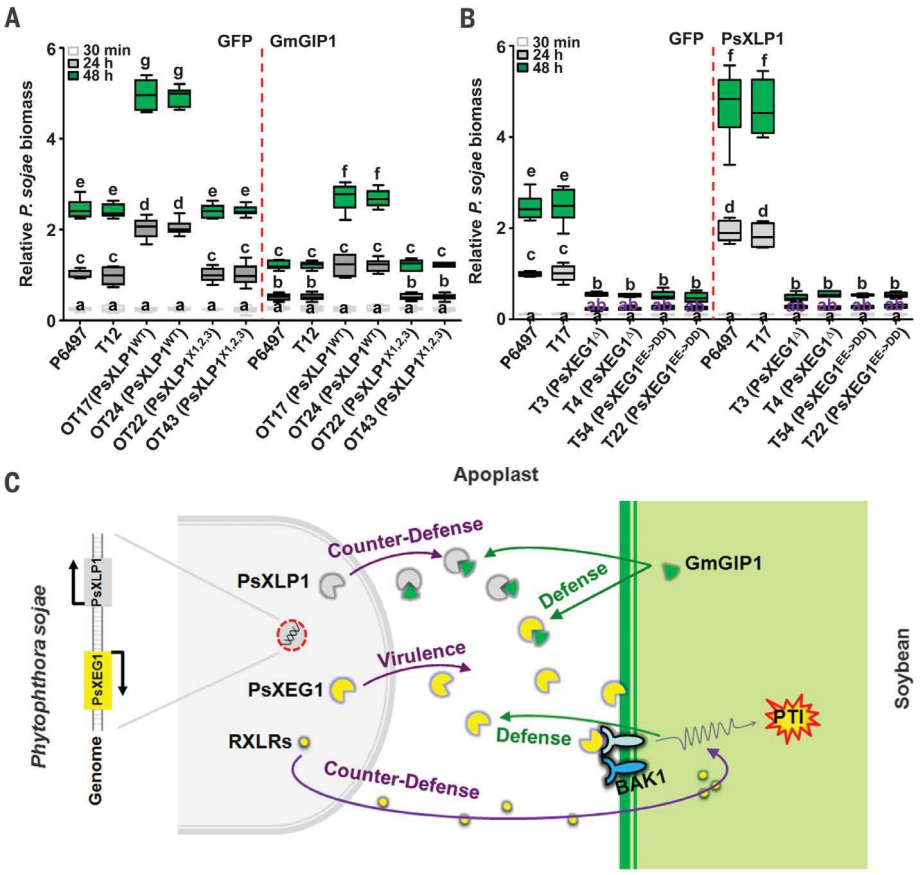

Fig. 4. Neutralization of GmGIP1-mediated defense by PsXLP1 is only observed in the presence of PsXEG1 during *P. sojae* infection of soybean hairy roots. (**A**) Overexpression of PsXLP1 in *P. sojae* neutralizes the defense provided by overexpression of GmGIP1 in transgenic soybean hairy roots. Shown is the relative biomass of wild-type and transgenic *P. sojae* in infected hairy roots expressing GmGIP1-GFP fusion protein, as measured by genomic DNA qPCR and normalized to wild-type *P. sojae* infection of hairy roots expressing GFP at 24 hpi. (**B**) PsXLP1 overexpression in hairy roots does not increase susceptibility to *P. sojae PsXEG1*-knockout lines. Shown is the relative biomass of *P. sojae* strains infecting transgenic hairy roots expressing GFP or PsXLP1-GFP fusion, measured as in (A). T17, control; *PsXEG1*$^{EE\rightarrow DD}$, *PsXEG1*$^{E136D,\ E222D}$ double mutant. In (A) and (B), experiments were replicated six times using 36 hairy roots from six different soybean cotyledons per biological replicate. Different letters represent significant differences ($P < 0.01$; Duncan's multiple range test). Bars represent medians, and boxes indicate the 25th and 75th percentiles. (**C**) Model for counterdefense by *P. sojae* against two distinct forms of PsXEG1-targeted plant defenses (PTI, PAMP-triggered immunity).

to the role of the interaction partner—initiation of defense in the case of a host, and protection of a virulence effector in the case of a pathogen.

It is interesting that NbGIP2 belongs to a different GIP clade than GmGIP1. Soybean (a rosid) and *N. benthamiana* (an asterid) diverged around 107 to 117 million years ago (*27*), whereas the genus *Phytophthora* is estimated to have radiated into different species around 20 million years ago (*28*). Thus, it is plausible that GmGIP1 and NbGIP2 evolved independently and convergently out of existing GIP superfamilies to counter the XEG1 weaponry of emerging *Phytophthora* pathogens. The substantial differences between GmGIP1 and NbGIP2 may explain why PsXLP1 and PpXLP1 have also evolved substantial differences.

Hosts and pathogens are engaged in a continuous evolutionary struggle for physiological dominance that determines the outcome of their interaction (*5*, *8*, *9*). One example is Ecp6, an apoplastic effector of *Cladosporium fulvum*, that shields pathogen-derived chitin fragments from recognition by host immune receptors (*29*, *30*). Here we have provided evidence that the essential apoplastic effector PsXEG1 and its homologs constitute a focal point of this coevolutionary struggle in diverse *Phytophthora*-plant pathosystems (*14*) (figs. S14 and S24) and that, at least in the *P. sojae*–soybean system, PsXEG1 is subject to two layers of defense and counterdefense (Fig. 4C). We previously showed (*14*) that recognition of PsXEG1 by soybean's PAMP recognition machinery has the potential to block *P. sojae* infection, but the PAMP-triggered immune response is in turn suppressed by multiple intracellular RxLR effectors. Here we have shown that PsXEG1 also is targeted by a second defense layer, an apoplastic inhibitor protein, GmGIP1, that can diminish the virulence of *P. sojae*, but that PsXEG1 is protected by its paralog, PsXLP1, which has evolved to bind more tightly than PsXEG1 to GmGIP1.

REFERENCES AND NOTES

1. S. Akira, S. Uematsu, O. Takeuchi, *Cell* **124**, 783–801 (2006).
2. C. Zipfel, *Trends Immunol.* **35**, 345–351 (2014).
3. J. D. Jones, J. L. Dangl, *Nature* **444**, 323–329 (2006).
4. T. Boller, S. Y. He, *Science* **324**, 742–744 (2009).
5. P. N. Dodds, J. P. Rathjen, *Nat. Rev. Genet.* **11**, 539–548 (2010).
6. L. Wirthmueller, A. Maqbool, M. J. Banfield, *Nat. Rev. Microbiol.* **11**, 761–776 (2013).
7. H. Rovenich, J. C. Boshoven, B. P. Thomma, *Curr. Opin. Plant Biol.* **20**, 96–103 (2014).
8. G. Doehlemann, C. Hemetsberger, *New Phytol.* **198**, 1001–1016 (2013).
9. L. Lo Presti *et al.*, *Annu. Rev. Plant Biol.* **66**, 513–545 (2015).
10. M. Latijnhouwers, P. J. de Wit, F. Govers, *Trends Microbiol.* **11**, 462–469 (2003).
11. S. Kamoun *et al.*, *Mol. Plant Pathol.* **16**, 413–434 (2015).
12. B. M. Tyler *et al.*, *Science* **313**, 1261–1266 (2006).
13. B. J. Haas *et al.*, *Nature* **461**, 393–398 (2009).
14. Z. Ma *et al.*, *Plant Cell* **27**, 2057–2072 (2015).
15. Q. Qin *et al.*, *Plant J.* **34**, 327–338 (2003).
16. T. Yoshizawa, T. Shimizu, H. Hirano, M. Sato, H. Hashimoto, *J. Biol. Chem.* **287**, 18710–18716 (2012).
17. Y. Fang, B. M. Tyler, *Mol. Plant Pathol.* **17**, 127–139 (2016).
18. S. C. Whisson *et al.*, *Nature* **450**, 115–118 (2007).
19. D. Mackey, Y. Belkhadir, J. M. Alonso, J. R. Ecker, J. L. Dangl, *Cell* **112**, 379–389 (2003).
20. P. Römer *et al.*, *Science* **318**, 645–648 (2007).
21. W. Xing *et al.*, *Nature* **449**, 243–247 (2007).
22. T. Xiang *et al.*, *Curr. Biol.* **18**, 74–80 (2008).
23. C. Zipfel, J. P. Rathjen, *Curr. Biol.* **18**, R218–R220 (2008).
24. M. Ilyas *et al.*, *Curr. Biol.* **25**, 2300–2306 (2015).
25. C. Le Roux *et al.*, *Cell* **161**, 1074–1088 (2015).
26. P. F. Sarris *et al.*, *Cell* **161**, 1089–1100 (2015).
27. M. J. Sanderson, J. L. Thorne, N. Wikström, K. Bremer, *Am. J. Bot.* **91**, 1656–1665 (2004).
28. N. H. Matari, J. E. Blair, *BMC Evol. Biol.* **14**, 101 (2014).
29. R. de Jonge *et al.*, *Science* **329**, 953–955 (2010).
30. P. J. de Wit, *Annu. Rev. Phytopathol.* **54**, 1–23 (2016).

ACKNOWLEDGMENTS

We thank W. Ma (University of California–Riverside) for helpful suggestions. This work was supported in part by grants to Yu.W. from the China National Funds for Distinguished Young Scientists (31225022), the Key Program of the National Natural Science Foundation of China (31430073), the Special Fund for Agro-scientific Research in the Public Interest (201303018), and the China Agriculture Research System (CARS-004-PS14); by a 111 International Cooperation grant (B07030) to Nanjing Agricultural University from the Chinese government; and by grants to B.M.T. from the National Research Initiative of the U.S. Department of Agriculture National Institute of Food and Agriculture (2011-68004-30104 and 2010-65110-20764). Y.F. is also supported by the Interdisciplinary Ph. D. Program in Genetics, Bioinformatics, and Computational Biology at Virginia Tech. Sequences have been deposited in GenBank under the submission accession numbers provided in the supplementary materials. The supplementary materials contain additional data.

SUPPLEMENTARY MATERIALS

www.sciencemag.org/content/355/6326/710/suppl/DC1
Materials and Methods
Figs. S1 to S24
Tables S1 to S7
References (*31*–*45*)
Data S1 to S6

13 August 2016; accepted 28 December 2016
Published online 12 January 2017
10.1126/science.aai7919

A paralogous decoy protects *Phytophthora sojae* apoplastic effector PsXEG1 from a host inhibitor

Zhenchuan Ma, Lin Zhu, Tianqiao Song, Yang Wang, Qi Zhang, Yeqiang Xia, Min Qiu, Yachun Lin, Haiyang Li, Liang Kong, Yufeng Fang, Wenwu Ye, Yan Wang, Suomeng Dong, Xiaobo Zheng, Brett M. Tyler and Yuanchao Wang (January 12, 2017)
Science **355** (6326), 710-714. [doi: 10.1126/science.aai7919]
originally published online January 12, 2017

Editor's Summary

Host-pathogen point-counterpoint

The arms race between pathogen and host is a well-known phenomenon. Ma *et al*. have now identified how an enzymatically inactive protein can abet a pathogen's infectivity. The pathogenic oomycete *Phytophthora sojae* secretes xyloglucanase that damages soybean cell walls. Soybean, in turn, secretes a defense protein that binds to and inactivates the xyloglucanase. To counteract this plant defense, the oomycete deploys a product of its own gene duplication: an inactive enzyme that binds the plant's defense protein. With the defense protein unproductively bound to the decoy, the oomycete can successfully invade the soybean cells.

Science, this issue p. 710

Science (print ISSN 0036-8075; online ISSN 1095-9203) is published weekly, except the last week in December, by the American Association for the Advancement of Science, 1200 New York Avenue NW, Washington, DC 20005.